Earth and Planetary Science Letters 519 (2019) 308–316

Contents lists available at ScienceDirect

Earth and Planetary Science Letters

www.elsevier.com/locate/epsl

Thin lithosphere beneath the central Appalachian Mountains: A combined seismic and magnetotelluric study

Rob. L. Evans [a,*], Margaret H. Benoit [b], Maureen D. Long [c], James Elsenbeck [a,d], Heather A. Ford [e], Jasmine Zhu [a], Xavier Garcia [f]

[a] Department of Geology and Geophysics, Woods Hole Oceanographic Institution, Woods Hole, MA 02543, USA
[b] The National Science Foundation, 2415 Eisenhower Avenue, Alexandria, VA 22314, USA
[c] Department of Geology and Geophysics, Yale University, New Haven, CT 06520, USA
[d] MIT Lincoln Labs, 244 Wood Street, Lexington, MA 02421-6426, USA
[e] Dept. of Earth Sciences, University of California, 900 University Ave, Riverside, CA 92521, USA
[f] Barcelona Center for Subsurface Imaging, Institute of Marine Sciences, CSIC, Barcelona, Spain

ARTICLE INFO

Article history:
Received 16 September 2018
Received in revised form 29 March 2019
Accepted 30 April 2019
Available online 27 May 2019
Editor: M. Ishii

Keywords:
magnetotellurics
seismic
receiver function
lithosphere

ABSTRACT

A joint analysis of magnetotelluric and Sp receiver function data, collected along a profile across the central Appalachians, highlights variations in regional lithospheric structure. While the interpretation of each data set by itself is non-unique, we identify three distinct features that are consistent with both the resistivity model and the receiver function image: 1) thin lithosphere beneath the Appalachian Mountains, 2) somewhat thicker lithosphere to the east of the mountains beneath the Coastal Plain, and 3) a lithosphere-asthenosphere boundary that deepens to the west of the mountains. In some regions, the correspondence between seismic velocity discontinuities and resistivity mark the base of the lithosphere, while in other locations we see seismic discontinuities that are contained within the lithosphere. At the western end of our profile a transition from highly resistive lithosphere to more conductive mantle represents the transition across the Grenville front. The thickness of lithosphere beneath the Grenville terrain is ~140 km. Lithosphere at the eastern end of the profile has a thickness that is not well constrained by our coverage, but is at least 110 km thick. This lithosphere can be associated with a broader region of high resistivity material seen to extend further south. Directly beneath the Appalachian Mountains, lithospheric thickness is inferred to be as thin as ~80 km, based on observations of elevated mantle conductivities and a westward-dipping seismic converter. Electrical conductivities in the uppermost asthenospheric mantle are sufficiently high (>0.1 S/m) to require the presence of a small volume of partial melt. The location of these elevated conductivities is close (offset ~50 km to the west) to Eocene volcanic outcrops in and around Harrisonburg, VA. Our observations speak to mechanisms of intraplate volcanism where there is no divergent or convergent plate motion to trigger mantle upwelling or obvious fluid release, either of which can facilitate melting. Instead, we suggest that small scale mantle convection related either to pre-existing lithospheric thickness variations, or to lithospheric loss through delamination, coupled with relative plate motion with respect to the underlying asthenosphere, can trigger small amounts of melting. This melt migrates upslope, along the base of the lithosphere, potentially thermally eroding the lithosphere resulting in further thinning.

1. Introduction

The central mid-Atlantic region of the Eastern North America Margin (ENAM) records a complex history of orogenesis and rifting. Intrinsically coupled to the rifting process is magmatic activity, most of which is thought to be contemporaneous with break-up and divergence. However, samples of volcanic outcrops in central Virginia describe two younger magmatic events that have impacted the region, one in the Jurassic (152 Ma) and one in the Eocene (47 Ma) (Mazza et al., 2014); this is significantly later than the last major stage of continental breakup and syn-rift magmatism, which occurred at ~190 Ma (Manspiezer et al., 1989; Holbrook and Kelemen, 1993). The Eocene magmatics are thought to be the output of a brief pulse that was of low volume, are bimodal in composition and have an equilibration depth of ~77 km. The magmas are relatively wet (1–3% wt% water) and are thought to derive

* Corresponding author.
E-mail address: revans@whoi.edu (R.L. Evans).

https://doi.org/10.1016/j.epsl.2019.04.046
0012-821X/

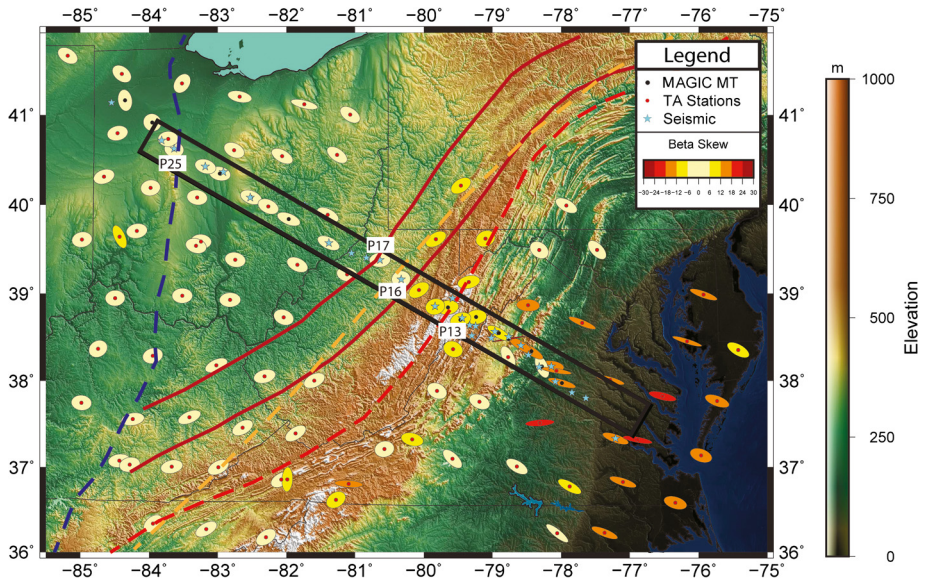

Fig. 1. A map of seismic and MT deployments of MAGIC and TA stations (Schultz et al., 2006-2018). The location of the primary MAGIC line lies within the black box. The phase tensor ellipses of each MT station at a period of 1196s (approximately sensing structure at mantle depths) are plotted and infilled by Beta-Skew values. The locations of MAGIC line seismic stations are shown by the blue stars. There is a clear gradient in Beta-skew and ellipticity, with values increasing towards the coastline. The blue line shows the approximate location of the Grenville Front, the red lines bracket the Rome Trough, the dashed orange line is the NY-AL lineament, and the red dashed line marks the Appalachian Front. (For interpretation of the colors in the figure(s), the reader is referred to the web version of this article.)

from asthenosphere beneath a dry lithospheric mantle. Mazza et al. (2014) argue that lithospheric thinning through delamination led to upwelling and subsequent melt generation. This model is supported by low seismic velocities seen in the upper mantle beneath the region (e.g., Schmandt and Lin, 2014; Porter et al., 2016; Wagner et al., 2018) from tomographic inversion of EarthScope Transportable Array seismic data.

The goal of this study is to interrogate the detailed present-day structure of the lithosphere beneath the central Appalachians, in the vicinity of the Eocene volcanic outcrops. Specifically, we combine constraints on lithospheric thickness obtained from electrical conductivity models (which delineate the contrast between highly conductive asthenosphere and highly resistive lithosphere) with those obtained from receiver function analysis (which delineate sharp contrasts in seismic impedance, as might be expected at the lithosphere-asthenosphere boundary). We rely mainly on data from the MAGIC experiment, which combined broadband seismic and magnetotelluric (MT) data acquisition with the aim of mapping the lithospheric structure through the crust and upper mantle. The experiment featured deployments of passive instrumentation along a profile from coastal Virginia to Ohio, crossing the Appalachian Mountains (Fig. 1.). The profile was proximal to the Eocene volcanic outcrops (Mazza et al., 2014). Seismometers and MT instruments were deployed at ∼25 km spacing along the profile. The majority of the seismometers were left in place for 2 years and recorded teleseismic arrivals that we use in this paper for construction of Sp receiver functions. In contrast, MT instruments required a 3-week deployment and provide a model of electrical resistivity through the continental lithospheric mantle and into the underlying asthenosphere. Like other recent studies in North America (e.g., Hopper and Fischer, 2018), we include data from the EarthScope Transportable Array and other permanent networks (US, N4); however the addition of the MAGIC data enables us to densify coverage in the region. Our goal is to identify variations in lithospheric thickness along the profile and to relate these variations to tectonic regime and processes in the asthenosphere, using a combination of receiver function analysis and resistivity models.

2. Central ENAM region

The break-up of Pangea and the formation of the Atlantic Ocean represents the final tectonic event to influence the lithosphere of the eastern U.S., although the region contains records of rifting events going back at least ∼1 Ga. This last rifting event began in the mid to late Triassic (Manspeizer et al., 1989), around 230 Ma, and was more intense in the north than in the south. Rifting was followed by a magmatic event culminating in the voluminous volcanism that accompanied continental breakup at ∼190 Ma, emplacing a ∼25 km thick combined plutonic and extrusive crustal section at the continent/ocean boundary along much of the North American margin (Holbrook and Kelemen, 1993). The Pangean rift-related Jurassic volcanic rocks are collectively referred to as the central Atlantic magmatic province, or CAMP (Marzoli et al., 2004).

A variety of seismic velocity models (e.g., van der Lee et al., 2008; Schmandt and Lin, 2014; Wagner et al., 2018) have been developed for eastern North America, the most recent of which take advantage of the dense coverage afforded by the EarthScope USArray Transportable Array (TA) (IRIS Transportable Array, 2003). An earlier shear-velocity model shows a dramatic and persistent low velocity anomaly roughly 300 km wide, parallel to the Appalachians (van der Lee et al., 2008). The anomaly starts at depths expected to be within the continental lithosphere and extends down to at least the 660 km discontinuity. The anomaly is somewhat controversial, largely because of its magnitude and extent, but a number of mechanisms for the anomaly are discussed, with the authors preferring extensive hydration of the mantle with the source of the fluids the relict Farallon slab. Water is known to lower mantle viscosity (Hirth and Kohlstedt, 1996) and so a wet region of mantle would be easier to break during rifting. A model of the entire continental United States, derived from TA data, shows a large and pronounced low-P wave velocity anomaly (Schmandt and Lin, 2014) that has become known as the Central Appalachian Anomaly (CAA). The anomaly sits beneath the location of Eocene volcanism and is, to some extent, coincident with the anomaly imaged by van der Lee et al. (2008). The spatial resolution of the model is poor in the uppermost ∼100 km of the mantle, both laterally and with depth, and so although a clear anomaly is seen, details of topography on the LAB and the relationship between

anomaly and the Appalachians are not well constrained. The seismic nature of the LAB beneath Eastern North America suggests a sharp velocity gradient inconsistent with a purely thermally controlled transition, with the suggestion that some combination of hydrous mantle and/or melt is present (Rychert et al., 2007; van der Lee et al., 2008).

More recent shear-wave velocity models, derived from Rayleigh wave data collected at TA stations, also show evidence for a low-velocity zone centered around the Eocene volcanics (Porter et al., 2016; Wagner et al., 2018). In the Wagner et al. (2018) model, low velocities begin just below the Moho, and spread over a region of roughly 100 km in diameter, although the size, location, and amplitude of the anomaly may be somewhat affected by parameterization, damping, and smoothing used in the inversions of the data. The Porter et al. (2016) model covers the continental US but clearly resolves a region of reduced velocities within the upper mantle to the east of the Grenville front. In both models the low velocities are consistent with the loss or modification of lithospheric mantle beneath this localized region.

Some additional seismic work has been done in the area of the MAGIC survey, particularly looking at anisotropy in the upper mantle through SKS splitting analysis (e.g., Long et al., 2016). A recent analysis of SKS splitting across the MAGIC array (Aragon et al., 2017) revealed small-scale lateral variations in splitting behavior, with stations within the Appalachian Mountains exhibiting fast splitting directions roughly parallel to the strike of the orogen. To the east, there is more complex splitting behavior, with a distinct clockwise rotation of fast directions and more null (that is, non-split) SKS arrivals.

3. Data and methods

3.1. MT data

Long-period MT data were collected at 25 sites which were occupied for ∼3 weeks. We used a combination of LEMI-417 owned by WHOI, and Narod Geophysics NIMS instruments made available by the National Geo-electromagnetic Facility at Oregon State University. Instrument recording units were housed in metal boxes for protection and deployed for ∼3 weeks. Siting was as close as possible to the location of seismic installations, although there are different noise criteria for MT and seismic stations and so in some cases, a new site had to be found. Details of the data processing are given in Supplementary Material.

In addition to our data-set, EarthScope TA MT acquisition passed through the area soon after we had completed our survey. These sites, at ∼70 km spacing on a 3D grid, allow us to embed our profile in a larger regional array and also provide some additional sites on our profile for 2D modeling. Data generally span the period band from 10 s to ∼10,000 s, with some variability in quality at either end of the period band. Phase-tensor ellipses (e.g., Caldwell et al., 2004) are shown for data at periods of 1196S in Fig. 1. These ellipses provide a graphical means of demonstrating the dimensionality of the impedance tensor. Near circular ellipses, with low skew values, are indicative of 1D resistivity structure beneath a station. As structure becomes more complex, the ellipticity increases. In the case of 2D structure, the major axis of the ellipse will align either parallel or perpendicular to the geo-electric strike direction, although the skew values will remain low. The data show varying levels of 3-dimensionality, with increasing values of ellipticity and Beta-Skew seen towards the coastline (Fig. 1), indicative of the polarization expected due to the conductive ocean. Elsewhere, however, ellipticity is quite low, as are skew values, leading us to conclude that a 2D inversion of data along the MAGIC profile should be a valid approach. However, we verify this assumption by first carrying out a 3D inversion of data collected at the stations shown in Fig. 1 in order to better assess the regional electrical structure, strike and continuity of conductive features in the area.

3.2. Seismic acquisition and analysis

The MAGIC seismic deployment (Fig. 1) was an EarthScope Flexible Array experiment consisting of 28 broadband seismometers deployed in a linear array across the central Appalachians, from Charles City, Virginia to Paulding, Ohio. Stations were deployed for periods ranging from 12 to 36 months between 2013 and 2016, with most stations deployed for 24 months. Nominal station spacing across the array was ∼25 km, with spacing as small as ∼10 km in the central portion of the array. Details of events utilized and processing methodology are given in Supplementary Materials, including a map of Sp pierce points at 210 km (Supplementary Fig. S7).

Receiver function (RF) analysis relies upon the principle that when an upward traveling wave (in this case, a shear wave) encounters a sharp change in velocity, some of the energy is converted to a compressional wave that can be measured at the Earth's surface. By stacking converted Sp arrivals that have a common conversion point (CCP), an image can be constructed that, in our case, reveals a number of features at mantle depths that reflect lateral variability in the structure of the mantle lithosphere (either its thickness or its internal structure). The interpretation of Sp receiver function CCP stacks is inherently ambiguous (e.g., Lekić and Fischer, 2017), and our interpretation of major features is done in the context of the MT model results, as described below.

4. Results

4.1. Resistivity model

Given that our profile is nested within the regional TA data coverage (Schultz et al., 2006-2018), we have carried out 3D inversions of our own data and TA data, both to assess regional structure and to assess the suitability of carrying out 2D inversions on the data collected along the MAGIC profile on their own. 2D inversion offers some computational advantages over 3D approaches, and it is more straightforward to carry out a comprehensive suite of sensitivity testing in 2D. The essential assumption in 2D, that resistivity is invariant along a pre-determined strike direction, does, however, place limitations on this approach. A regional 3D model allows us to determine the along strike continuity of key features as well as to identify their orientation.

We ran a suite of 3D inversions (see Supplementary Material for details) with differing smoothing parameters, paying particular attention to setting appropriate (and different) values for the crust and mantle. In runs with uniform regularization, the resulting models were highly vertically smeared with crustal conductors "dripping" down into the mantle. We also examined fits to the data post-inversion and excluded data that were clearly outliers before re-running another round of inversion iterations. In most cases where a significant misfit was experienced, the misfit was largely the result of static shift effects, with the trend of the response matching that of the data. Assessment of the fit of the model to the data was carried out by viewing misfit maps (Supplementary Fig. S1), with misfit calculated for each station and also for each component of the impedance tensor. It is important that poor misfit not be concentrated in one region of the model, or over a specific period band.

Having carried out a series of inversions, we arrive at models with global misfit values in the range of 1.7–2.26, with the lowest misfit model having a large amount of small scale structure at all depths that is likely the result of overfitting the data. The

model with misfit of 2.26 is our preferred 3D model (Supplementary Figs. S2 and S3a), although the primary features in the mantle are consistent between inversions.

The 3D model contains a series of features, but the most important is a conductor which begins to take a continuous form at around 100 km depth (Supplementary Figs. S2 and S3a). At depths between ∼125–175 km, this feature bifurcates around the location of the MAGIC line from a single conductor into two, one with a ∼ northerly strike (C1) and one with a strike of ∼45 degrees (C2). C2 is the most pronounced feature to depths of ∼150 km, while C1 appears continuous to greater depth. We have chosen a strike direction aligned roughly with the single feature south of our profile and of C2 for the purposes of 2D modeling, but with the understanding that the 2D inversion will have to account for the two different striking features. This will likely result in differences in the locations and magnitudes of features at depth between the 2D and 3D model.

We have recovered a suite of 2D models that provide a satisfactory fit to the data (details in Supplementary Material). In running 2D inversions, a primary consideration is the trade-off between fitting the data well and introducing spurious structure. This trade-off is controlled by a regularization parameter, τ. We ran a series of inversions with a wide range of smoothness constraint values (τ) logarithmically spaced between 0.001 and 100 to find the models that best minimize misfit without introducing unrealistic or unnecessary structure. Other regularization parameters that can be varied place different emphasis on horizontal or vertical structure. There is no single optimal choice of regularization parameters, but rather we see consistent structure between models with a wide range of parameters. We have chosen a representative 2D model that contains quite smooth versions of these features (Fig. 2a), and which was derived using a τ of 3.0. Features that appear in only small subsets of the returned models are not considered robust and are not further discussed. The range of misfits returned for what we consider to be acceptable models range from 1.5 to 1.7. Inversions of the Tipper data alone return a model that fits the data very well (RMS misfit of less than 1.0) with similar features to the inversion of the full MT data set.

Although there are always subtle differences in models created by inversions with different settings, our models (both from 2D and 3D inversions) show some common first-order features. Testing for sensitivity of the data to particular features is more straightforward to accomplish in the 2D analysis. Details of how these tests have been done are given in Evans et al. (2011) (reproduced in Supplementary Material). This process involves running hundreds of inversions and forward models in order to arrive at robust conclusions. In discussing the results of our modeling we focus on these first order features and below we discuss which facets of each we consider well resolved. These features are:

1. A region of resistive material at the western end of the profile.

The resistive structure at the western end of the profile is ∼140–160 km thick. The mantle immediately to the east side of the highly resistive structure is more conductive than expected for lithospheric mantle.

2. A thicker and more resistive body at the eastern end of the profile.

There is another region of resistive mantle to the east of the array. The depth extent of the resistor is not well constrained by the data, and it can be as thin as ∼110 km or as thick as ∼200 km. The resistors in the 3D model extend to greater depth than in the 2D model, but this is not required by the data and resistive thicknesses consistent with the 2D model fit the data equally well.

3. A transition to highly conductive asthenosphere beneath the region to the west of the Appalachians.

Between the two regions of deep high resistivity, the mantle is more conductive, with two highly conductive regions of the uppermost asthenosphere. This structure is suggestive of thinned lithosphere. Beneath the mountain belt, lithospheric thickness appears to be as small as ∼80 km, but thickens to the west. We have specifically tested this thickening and our inference of the LAB depth (Fig. 2e) based on resistivity and present details in Supplementary Material. The two regions of high conductivity are centered at depths of approximately 170 km and 220 km in the 2D model, but are roughly 50 km shallower in the 3D model. However, the depth at which conductivity starts to increase is about the same in both sets of models. The deeper conductors are elongated along strike, justifying the 2D assumption. However, the strikes of the two conductive features in the 3D model are different to one another, a complexity that the 2D model has to accommodate, with the result that the geometries of conductors, and their position along-profile, are slightly different. Conductivities in the upper asthenosphere are sufficiently high (∼ a few Ohm-m) to require the presence of partial melt. This inference of thin lithosphere is consistent with results from Sp receiver functions, as discussed in section 4.2.

Fig. 2c shows a cross section from the Porter et al. (2016) shear velocity model along the MAGIC profile. The figure clearly demonstrates the lower resolution of the velocity model compared to the resistivity models, but it also clearly shows that velocities are significantly reduced over a substantial volume of mantle beneath the mountains, but with faster velocities in the upper-mantle to the west. The somewhat reduced velocities to the east of the mountain belt are, taken at face value, contradictory to the resistivity models. However, we are confident that there is a sharp transition to resistive structure in this region of our models.

4. Models contain various geometries of mid-lower crustal conductors.

There are a variety of explanations given for crustal conductors, ranging from aqueous fluids, melts through to conductive solid phases such as sulphide and graphite. We explore these below in the context of the Appalachian region.

4.2. Sp receiver function results

A 2D slice along the MAGIC line through the 3D stacked CCP image of Sp receiver function data is shown in Fig. 2. In addition to this figure, in the Supplementary Material we show cross sections through the 3D MT model with Sp RF amplitudes superimposed (Supplementary Fig. S2), as well as an animation showing co-registered slices through both the 3D MT model and the 3D CCP volume (Supplementary Material animation file). Here we focus our interpretation on features that are consistent with a decrease in velocity with depth, which may correspond to the base of the lithosphere (lithosphere-asthenosphere boundary, or LAB; see, e.g., Rychert et al., 2007) or to the so-called mid-lithospheric discontinuity (MLD) (e.g., Ford et al., 2010, 2016; Hopper and Fischer, 2015). At the eastern end of the MAGIC profile (Fig. 1), we observe multiple negative discontinuities (Features A1 and A2 in Fig. 2b), with an intermittent converter at a depth of ∼70 km (mainly visible at the very edge of the profile, where the reduction in piercing point event density is significantly lower and therefore receiver function signal-to-noise quality is reduced) and another converter at a depth of ∼110 km. The deeper of these may correspond to the LAB, although this association is tentative, and is based in part on comparison with features of the resistivity model (discussed above) as well as with previously published tomography models of shear wave velocity (Schmandt and Lin, 2014; Wagner et al., 2018).

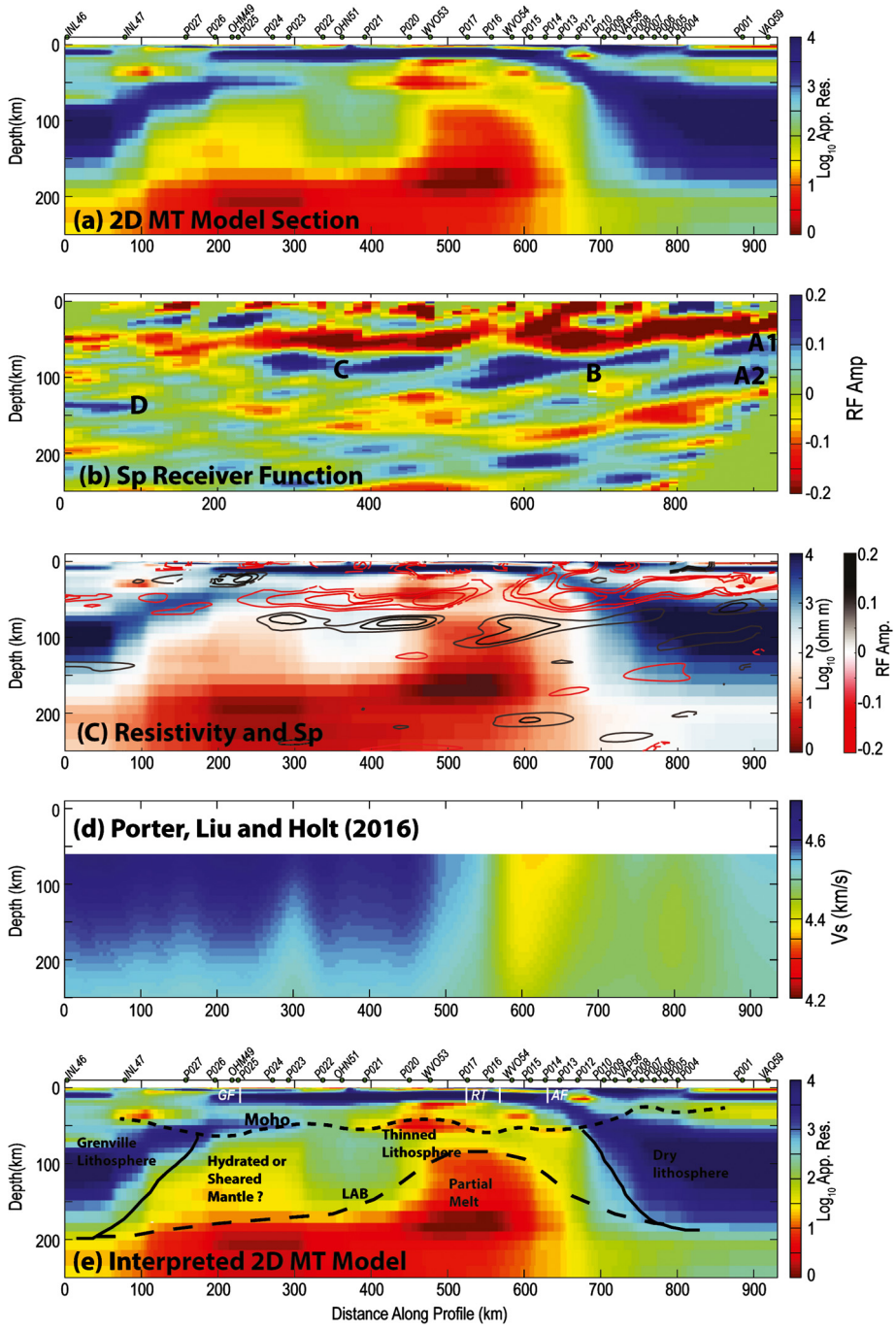

Fig. 2. Cross sections of models along the MAGIC profiles. (a) The preferred 2D MT model; (b) Sp receiver function image with key Features A-D as discussed in the text; (c) the 2D MT model with SP receiver functions overlain. The MT model is shown on a different color scale for clarity and the receiver functions are thresholded to show primary features; (d) the shear velocity model of Porter et al. (2016); (e) an interpreted view of the 2D model highlighting primary features discussed in the text. The approximate surface locations of the Grenville Front (GF), Rome Trough (RT) and Appalachian Front (AF) are shown by the white lines as labeled. The sections run from the west (0 km distance along profile) to east, with the Atlantic coast on the right.

Moving along the profile, we observe a strong and clearly imaged negative discontinuity beneath the high Appalachian topography, extending into western West Virginia (Feature B in Fig. 2b). This feature is located at a depth of ∼70–80 km at its eastern end, and dips to the west, to a depth of ∼130 km at its western end. Based on correspondence between this discontinuity and features in the resistivity model (Fig. 2c), specifically the significant decrease in resistivity, we interpret this dipping converter as the LAB beneath the Appalachian Mountains, suggesting notably thin lithosphere beneath this region. Hopper and Fischer (2018) analyzed Sp phases from TA stations in the same area and documented that a localized velocity drop of more than ∼6.5% ± 4% was required to generate the observed phases. They further argued that such a large drop cannot be due to purely thermal gradients, nor to water in olivine, but instead suggests some degree of partial melt in the mantle.

Beneath the western third of our profile, we image a strong, flat negative converter at a depth of ∼90 km (Feature C in Fig. 2b). Given that seismic velocities at this depth range in this region are relatively fast (e.g., Wagner et al., 2018; Porter et al., 2016; Fig. 2c), we infer that this discontinuity lies within the mantle lithosphere and thus corresponds to an MLD. Finally, in the westernmost part

of the MAGIC profile, we observe intermittent converters at depths between ∼140–170 km (Feature D in Fig. 2b). Although this discontinuity is weaker and less well defined than other features in the CCP stack, there is at least a hint that it may represent the continuation of the dipping LAB (Feature B in Fig. 2b) beneath the Appalachian Mountains to the west. This interpretation would be consistent with features of the resistivity model; if correct, then this feature may represent the gradual thickening of the lithosphere to the west of our study area, with the thickest lithosphere (LAB depth of ∼130 km) roughly in the vicinity of the Grenville Front.

We emphasize that the interpretation of the RF image in Fig. 2b is non-unique, and alternative interpretations are possible. For example, we cannot exclude the possibility that Features A1 and B are actually a continuous feature representing the LAB; nor can we rule an alternative interpretation of Feature C as the LAB rather than an MLD. In the context of the constraints provided by the MT model, however, these alternative interpretations are less likely; the combination of constraints from multiple geophysical imaging techniques thus helps to overcome the non-uniqueness of the RF imaging.

5. Interpretation and discussion

5.1. Crustal components

The seismic receiver function data clearly delineate the Moho across the profile, although with the generally lower frequency content of Sp receiver function data when compared to Ps data, the detailed structure of the Moho is obscured in the Sp CCP image. The nominal Moho depths suggested by the Sp RF observations range from ∼30 km at the eastern end of the seismic array to ∼50–55 km beneath the highest Appalachian topography and beneath central Ohio. These crustal thickness estimates are generally consistent with those obtained via Ps RF analysis, described elsewhere (Long et al., 2019).

Our resistivity models have a number of conductive features within the crust. Although the geometry of these features differs between models, there is broad agreement between the locations of these conductors and significant crustal boundaries as delineated by magnetic data. For example, the New York–Alabama (NY-AL) (Fig. 1) lineament is a large and continuous magnetic anomaly that is thought to represent the location of a crustal suture (Steltenpohl et al., 2010). COCORP seismic reflection profiling highlights the Coshocton zone, a ∼100 km wide, 30 km deep, western dipping feature in which the reflection patterns are believed to arise from shear fabrics developed in a metasedimentary belt associated with suturing (Culotta et al., 1990).

Elsewhere, such regions of heavily deformed metasediments have been correlated with high crustal conductivities, with high conductivities arising from well connected sulphides, graphite or other minerals (e.g., Jones et al., 1997). An example from the North American Central Plains (NACP) conductivity anomaly (Jones et al., 1997), shows elevated conductivities related to this effect. However, electrical anisotropy is also observed (2–3 orders of magnitude), which is greater than we see in this survey (see Supplementary Material for discussion), although we reiterate that our survey design is not optimized for providing constraints on crustal structure.

A large conductor associated with the Grenville suture is reported by Wannamaker (2005). Again, this conductor is associated with anisotropic electrical structure and is concentrated in the crust, although the high conductivity appears to bleed into the mantle. The high conductivity is interpreted to result from the underthrusting of graphite-bearing metasediments as part of the collisional suture.

Evidence for sulphides in the crust can be found in the eastern portions of the survey area, in what is known as the Mineral District, Virginia which features a band of metalliferous deposits. This band sits between sites 3 and 4 (Sandhaus and Craig, 1986) and is perhaps connected to a volcanic-plutonic belt and associated sulfides (Robinson et al., 1988), just to the west around sites 5 and 6, where we see a shallow crustal conductor. This feature is, however, quite different than the deeper conductors west of the Appalachians.

Melt in the crust?

Elevated heat flow is seen across the Appalachians, with values of between 70–80 mW/m^2 across the mountains (Frone et al., 2015). Analysis of heat flow and borehole temperature analysis shows evidence for a gradient in thermal structure from west to east, with higher thermal gradients with depth inferred beneath the Appalachians (Frone et al., 2015). Numerical modeling suggests that heat flow is uniform at the base of the sedimentary basin associated with the Rome trough, which runs to the west of the mountain belt. The authors suggest that variations in sediment thermal properties, and perhaps fluid flow, might be responsible for surface variations in heat flow. However, our observed lithospheric structure, coupled with seismic observations of thickened crust beneath the mountains (Long et al., 2019), suggest that deeper processes might be responsible for generating heat at depth.

Although high for a continental setting, the heat flow values in this region are lower than those seen across the Rocky Mountains, where values in excess of 100 m mW/m^2 have been observed (Decker et al., 1988), but are in line with those seen in the North-Central Colorado Plateau (Bodell and Chapman, 1982). This latter comparison is important, as the Eastern Great-Basin marks a similar location of thinned lithosphere with asthenospheric melt and lower crustal conductors imaged using MT (Wannamaker et al., 2008). In this case, the lower crustal conductors are attributed to a combination of melts and hot saline fluids.

The conductors to the west of the Appalachians have a clear vertical separation from the conductive asthenosphere, and we attribute these to mineralization related to tectonic deformation and shearing of metasediments. It is possible, however, that elevated conductivities in the lower crust beneath the Appalachians are caused by a combination of melts and saline fluids.

5.2. Mantle structure

MT models consistently show a conductive region of mantle that shoals to the east, with a shallowest depth of ∼80 km beneath the Appalachian Mountains (Fig. 2; Supplementary Fig. S2). These models are consistent with a loss of lithosphere beneath this region of the Appalachians and to the west. Conductivities are sufficiently high in the uppermost asthenosphere to be consistent with the presence of a small volume of partial melt: they cannot be explained simply by raised temperatures. There is an obvious spatial connection between the thinnest region of lithosphere and the location of Eocene volcanic outcrops (Mazza et al., 2014). One plausible interpretation of the receiver function images supports this model, with an observed shallow, westward-dipping converter (Feature B in Fig. 2b) that is broadly coincident with the transition from resistive to conductive mantle in the MT model. Other features observed in the RF profiles occur in regions of high electrical resistivity; therefore, we interpret them jointly with the MT model as corresponding to mid-lithospheric discontinuities.

Seismic tomography models from the regions, which have lower resolution than our MT model, show reduced seismic velocities in the upper asthenosphere (Schmandt and Lin, 2014; Porter et

al., 2016; Wagner et al., 2018) which has been interpreted as evidence for lithospheric delamination and subsequent upwelling and melting of the mantle. Our MT models all consistently and robustly contain a region of high conductivity at depths beneath ~150 km in the center of our profile (Fig. 2), generally consistent with the observed velocity anomalies, although the location of the strongest conductivity anomaly is deeper and to the west of the strongest seismic velocity anomalies (Fig. 2c) (Schmandt and Lin, 2014; Porter et al., 2016; Wagner et al., 2018). Similarly, Byrnes et al. (2019) show clear evidence for high seismic attenuation beneath the mountains from analysis of teleseismic P waves collected on the MAGIC line. This high attenuation anomaly is concentrated in a ~100 km wide region, spatially coincident with the shallow mantle conductivity feature in the MT model, and likely requires some level of partial melt in the upper-mantle. Our interpretation of thin lithosphere beneath the Appalachian Mountains based on MT and RF observations is thus consistent with independent lines of evidence from seismic tomography and attenuation models.

We note the geographical coincidence between the region with thin lithosphere we infer here and stations that exhibit particularly anomalous SKS splitting, as documented in Aragon et al. (2017), with a pronounced rotation in fast directions and an increase in the complexity of splitting patterns at individual stations. A comparison of SKS splitting delay times (δt) at MAGIC stations located above the anomalously thin lithosphere and δt documented at TA stations in the Appalachian Mountains to the south and west of the MAGIC line (Long et al., 2016) reveal reduced δt associated with thin lithosphere. This observation is consistent with previous interpretations that SKS splitting in the Appalachians reflects a component of frozen-in anisotropy in the lithospheric mantle associated with Appalachian orogenesis (Long et al., 2016; Aragon et al., 2017); beneath the MAGIC line, the thinned lithosphere results in smaller δt.

The resistive region in the western portion of the profile is suggestive of thicker lithosphere associated with the Grenville front. Lithospheric thickness to the east is not well constrained, as we have only a few stations in this part of the profile. Our models here are consistent with a lithospheric thickness of 110–120 km, although models with much thicker resistive lithosphere in this region also satisfy the data. Models with thicker lithosphere are similar to that of Murphy and Egbert (2017) who use TA data from the southeastern US to image a large, thick resistive feature beneath the coastal plain from northern Florida into Virginia. This feature is controversial, as seismic velocity models do not show commensurate fast velocities (Wagner et al., 2018) which would be expected for a cool, dry block of lithospheric mantle (e.g., Jones et al., 2013).

Origin and evolution of thinned lithosphere

By themselves, our data cannot identify the origin of the thinned lithosphere. One suggestion has been that a piece of lithospheric mantle delaminated, resulting in upwelling and melting (Mazza et al., 2014). This model might be consistent with the suggestion that the mantle beneath the Appalachians is hydrous (e.g., van der Lee et al., 2008), leading to a reduction in viscosity and strength. Another possibility is that variable topography on the base of the lithosphere post-rifting generated mantle upwelling as a result of shear-induced flow (e.g., Conrad et al., 2011). Melt would migrate upslope along the base of the LAB, ponding at the shallowest point. Once there, it is possible for melt to thermally erode the lithosphere through processes of dike intrusion. Havlin et al. (2013) present models with modest melt fractions capable of thinning ~50 km of lithosphere or more over a 50 Ma time frame. This model is attractive as it does not require a significant delamination event to occur prior to melt accumulation, but rather just a modest topography on the LAB. Similar inferences of thermal erosion of the lithosphere by melt migration have been made elsewhere in continental settings (e.g., Ford et al., 2010; Evans et al., 2019). Various styles of continental lithosphere removal have been interrogated via numerical modeling (e.g., Beall et al., 2017), and the resulting magmatic expressions have also been explored (e.g., Wang and Currie, 2015). It remains difficult, however, to diagnose a particular style of lithospheric removal, or to characterize how the lithospheric structure has evolved through time, by examining geophysical images of the present-day lithospheric structure. Detailed and regionally specific models of the Central Appalachians, guided by the images presented here, will be needed to understand the plausible mechanisms for lithospheric evolution, and predict how it might continue to evolve in the future.

Our results raise the question of how common lithospheric removal beneath rifted passive margins might be, and why the lithospheric modification we infer beneath the Central Appalachians is not more widespread beneath eastern North America. In the Appalachian system this process appears to be limited to this location and to beneath New England (Menke et al., 2018), where the similarly large North Appalachian Anomaly (NAA) is also thought to be related either to removal lithosphere or to a delamination event. There is debate, however, about whether the NAA is a young feature or whether it may be related to the passage of the Monteregian hotspot (see, e.g., Levin et al., 2018; Menke et al., 2018). At this point it is not well understood what controls the distribution, in both space and time, of lithospheric removal beneath the eastern North American margin, but this represents a key open question for future work.

Water and melt in the mantle?

The primary factors that can elevate conductivity in the mantle, aside from elevated temperature, are water dissolved in olivine and partial melt. The magnitude of the effect of water on bulk mantle conductivity has been widely discussed and is controversial, as various labs have reported differing results. Naif (2018) shows upper-bounds on mantle conductivities based on the various published results for hydrous olivine conductivity. Although these are presented for oceanic geotherms, we can reasonably argue that the regions of mantle to the east of the Grenville Front with resistivities of around 30–100 Ω-m are consistent with a hydrated composition. Resistivities less than ~10 Ω-m likely require the presence of melt, especially in the asthenosphere where water storage capacity is reduced (Ferot and Bolfan-Casanova, 2012). A similar conclusion was made by Feucht et al. (2017) who collected data across the Rocky Mountain transition in Colorado and imaged a transition from resistive continental lithosphere to moderately conductive mantle.

Assuming melt in the present-day upper mantle has similar composition to the erupted Eocene volcanics (Mazza et al., 2014), which are largely basaltic, we estimate the conductivity of the melts to be around 1.3–1.7 S/m at 1300 °C (Pommier and Le Trong, 2011). However, Pommier and Garnero (2014) show that at the initiation of melting, the silicate melts produced have higher Na_2O content, which drives their conductivities up by a factor of 5. Conductivity values in excess of 10 S/m, and as high as 20 S/m are entirely possible. Melt fraction estimates, assuming an ideally interconnected network and based on melt conductivities in the 1.3–1.7 S/m range, would be quite high (7–10%) and would increase with depth, which is not reasonable. However, assuming a gradient in conductivity (as well as temperature) with depth to reflect the fact that the onset of melting is deeper, then melt factions in the asthenosphere could be as low as ~0.8%.

Shearing has also been shown to elevate olivine conductivity, perhaps as a result of increasing grain boundary conduction pro-

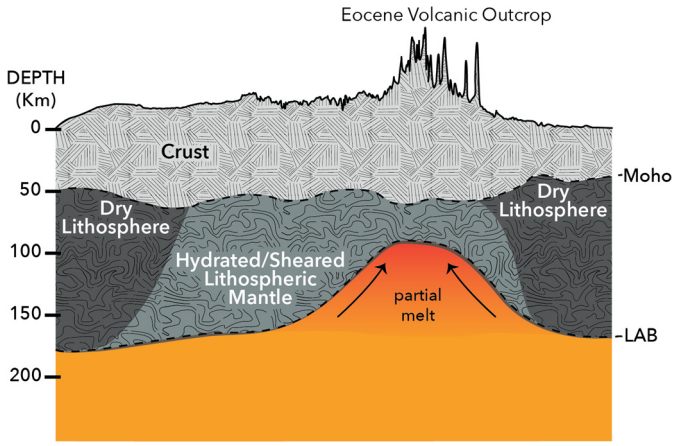

Fig. 3. A schematic cartoon of the key tectonic elements inferred from our model.

cesses. Achieving resistivities of between 30 and 100 Ω-m, such as are seen in the lithospheric mantle to the east of the Grenville Front, would require temperatures to be above ∼1150 °C (Pommier et al., 2018). However, the presence of a deeper conductor in the asthenosphere to the east of the Grenville Front might point to some trace-level of upward melt migration into the mantle in this region.

6. Conclusions

This study presents lithospheric thickness estimates across the central Appalachians from a joint interpretation of an electrical resistivity model and an image derived from Sp RFs. While the resistivity and RF models differ in many of their details, and on their own present some degree of ambiguity in interpretation, taken together both results are consistent with the presence of thin lithosphere beneath the Appalachian Mountains, somewhat thicker lithosphere to the east beneath the Coastal Plain, and gradually thickening lithosphere to the west of the mountains. The region of lithospheric thinning beneath the Appalachians is spatially associated with localized Eocene magmatism in the region around Harrisonburg, Va. Fig. 3 shows a cartoon summarizing the key features in the mantle inferred from our models. Both Sp receiver function constraints and electrical conductivity models strongly suggest a lithosphere as thin as ∼80 km beneath the Appalachian Mountains. Mantle conductivities are sufficiently elevated to require the presence of a small amount of partial melt. The volume of melt needed is dependent on melt composition and temperature, but for a reasonable range of likely melt compositions. We estimate that melt fractions less than ∼1% can give rise to the anomalies seen. More significant than the volume of melt present is the net effect on lithospheric structure that we infer has been caused by the sustained presence of melt in the mantle beneath this region, with lithosphere that has been thermally eroded over a period of at least 50 Ma. This study demonstrates the promise of combining multiple geophysical imaging techniques to study the structure of the continental lithosphere. In this case, the combination of MT and receiver function constraints allows us to identify a model that can simultaneously satisfy both observations, even though the interpretations of the individual data sets are non-unique.

Acknowledgements

Both seismic and MT data from the USArray Transportable Array (network code: TA) and MAGIC Flexible Array (network code: 7A; dois: 10.7914/SN/7A_2013 and 10.17611/DP/EMTF/MAGIC) were used in this study and can be downloaded from the Incorporated Research Institutions for Seismology (IRIS) Data Management center (DMC) at http://ds.iris.edu. Seismic instruments were provided by the IRIS PASSCAL Instrument Center at New Mexico Tech. The facilities of the IRIS Consortium are supported by the National Science Foundation under Cooperative Agreement EAR-1261681 and the DOE National Nuclear Security Administration. Seismic data acquisition and analysis was supported by NSF grant EAR-1251515 to Yale University and grant EAR-1251329 to the College of New Jersey. MT data were collected under NSF grant EAR-1460257 to WHOI, using instruments provided by the EarthScope program and maintained by Oregon State University. We are grateful to the many landowners and partner universities who hosted stations or provided logistical support. This work benefited from discussions at the EarthScope Synthesis Workshop on the Evolution of the Southern Appalachian Lithosphere in March 2017. The NSF I/D program helped support preparation of this manuscript. Any opinion, findings, and conclusions or recommendations expressed in this article are those of the authors and do not necessarily reflect the views of the National Science Foundation.

Appendix A. Supplementary material

Supplementary material related to this article can be found online at https://doi.org/10.1016/j.epsl.2019.04.046.

References

Aragon, J.C., Long, M.D., Benoit, M.H., 2017. Lateral variations in SKS splitting across the MAGIC array, central Appalachians. Geochem. Geophys. Geosyst. 18, 4136–4155. https://doi.org/10.1002/2017GC007169.

Beall, A.P., Moresi, L., Stern, T., 2017. Dripping or delamination? A range of mechanisms for removing the lower crust or lithosphere. Geophys. J. Int. 210, 671–692.

Bodell, J.M., Chapman, D.S., 1982. Heat flow in the north-central Colorado Plateau. J. Geophys. Res., Solid Earth 87, 2869–2884.

Byrnes, J.S., Bezada, M., Long, M.D., Benoit, M.H., 2019. Thin lithosphere beneath the central Appalachian Mountains: constraints from seismic attenuation beneath the MAGIC array. Earth Planet. Sci. Lett. 519, 297–307. https://doi.org/10.1016/j.epsl.2019.04.045.

Caldwell, T.G., Bibby, H.M., Brown, C., 2004. The magnetotelluric phase tensor. Geophys. J. Int. 158 (2), 457–469.

Conrad, C.P., Bianco, T.A., Smith, E.I., Wessel, P., 2011. Patterns of intraplate volcanism controlled by asthenospheric shear. Nat. Geosci. 4 (5), 317–321.

Culotta, R.C., Pratt, T., Oliver, J., 1990. A tale of two sutures: COCORP's deep seismic surveys of the Grenville province in the eastern US midcontinent. Geology 18 (7), 646–649.

Decker, E.R., Heasler, H.P., Buelow, K.L., Baker, K.H., Hallin, J.S., 1988. Significance of past and recent heat-flow and radioactivity studies in the Southern Rocky Mountains region. Geol. Soc. Am. Bull. 100 (12), 1851–1885.

Evans, R.L., Jones, A.G., Garcia, X., Muller, M., Hamilton, M., Evans, S., Fourie, S., Spratt, J., Webb, S., Jelsma, H., Hutchins, D., 2011. The electrical lithosphere beneath the Kaapvaal Craton, Southern Africa. J. Geophys. Res. 116. https://doi.org/10.1029/2010JB007883.

Evans, R.L., Elsenbeck, J., Zhu, J., Abdelsalam, M.G., Sarafian, E., Abdelsalam, M.G., Mutamina, D., Chilongola, F., Atekwana, E., Jones, A.G., 2019. Structure of the lithosphere beneath the Barotse Basin, SW Zambia, from magnetotelluric data. Tectonics 38 (2), 666–686. https://doi.org/10.1029/2018TC005246.

Ferot, A., Bolfan-Casanova, N., 2012. Water storage capacity in olivine and pyroxene to 14 GPa: implications for the water content of Earth's upper mantle and nature of seismic discontinuities. Earth Planet. Sci. Lett. 349–350, 218–230. https://doi.org/10.1016/j.epsl.2012.06.022.

Feucht, D.W., Sheehan, A.F., Bedrosian, P.A., 2017. Magnetotelluric imaging of lower crustal melt and lithospheric hydration in the Rocky Mountain Front transition zone. J. Geophys. Res. 122 (12), 9849-9510. https://doi.org/10.1002/2017JB014474.

Ford, H.A., Fischer, K.M., Abt, D.L., Rychert, C.A., Elkins-Tanton, L.T., 2010. The lithosphere-asthenosphere boundary and cratonic lithospheric layering beneath Australia from Sp wave imaging. Earth Planet. Sci. Lett. 300, 299–310. https://doi.org/10.1016/j.epsl.2010.10.007.

Ford, H.A., Long, M.D., Wirth, E.A., 2016. Mid-lithospheric discontinuities and complex anisotropic layering in the mantle lithosphere beneath the Wyoming and Superior provinces. J. Geophys. Res., Solid Earth 121. https://doi.org/10.1002/2016JB012978.

Frone, Z.S., Blackwell, D.D., Richards, M.C., Hornbach, M.J., 2015. Heat flow and thermal modeling of the Appalachian Basin, West Virginia. Geosphere 11 (5), 1279–1290.

Havlin, C., Parmentier, E.M., Hirth, G., 2013. Dike propagation driven by melt accumulation at the lithosphere–asthenosphere boundary. Earth Planet. Sci. Lett. 376, 20–28.

Hirth, G., Kohlstedt, D.L., 1996. Water in the oceanic upper mantle: implications for rheology, melt extraction and the evolution of the lithosphere. Earth Planet. Sci. Lett. 144, 93–108.

Holbrook, W.S., Kelemen, P.B., 1993. Large igneous province on the US Atlantic margin and implications for magmatism during continental breakup. Nature 364, 433–436.

Hopper, E., Fischer, K.M., 2015. The meaning of midlithospheric discontinuities: a case study in the northern U.S. craton. Geochem. Geophys. Geosyst. 16, 4057–4083. https://doi.org/10.1002/2015GC006030.

Hopper, E., Fischer, K.M., 2018. The changing face of the lithosphere-asthenosphere boundary: imaging continental scale patterns in upper mantle structure across the contiguous U.S. with Sp converted waves. Geochem. Geophys. Geosyst. 19 (8), 2593–2614. https://doi.org/10.1029/2018GC007476.

IRIS Transportable Array, 2003. USArray Transportable Array. International Federation of Digital Seismograph Networks. Other/Seismic Network. https://doi.org/10.7914/SN/TA.

Jones, A.G., Katsube, T.J., Schwann, P., 1997. The longest conductivity anomaly in the world explained: sulphides in fold hinges causing very high electrical anisotropy. J. Geomagn. Geoelectr. 49 (11–12), 1619–1629.

Jones, A.G., Fishwick, S., Evans, R.L., Muller, M.M., Fullea, J., 2013. Velocity-conductivity relations for cratonic lithosphere and their application: example of Southern Africa. Geochemi. Geophys. Geosyst. https://doi.org/10.1002/ggge.20075.

Lekić, V., Fischer, K.M., 2017. Interpreting spatially stacked Sp receiver functions. Geophys. J. Int. 210 (2), 874–886. https://doi.org/10.1093/gji/ggx206.

Levin, V., Long, M.D., Skryzalin, P., Li, Y., López, I., 2018. Seismic evidence for a recently formed mantle upwelling beneath, New England. Geology 46, 87–90.

Long, M.D., Jackson, K.G., McNamara, J.F., 2016. SKS splitting beneath Transportable Array stations in eastern North America and the signature of past lithospheric deformation. Geochem. Geophys. Geosyst. 17, 2–15. https://doi.org/10.1002/2015GC006088.

Long, M.D., Benoit, M.H., Aragon, J.C., King, S.D., 2019. Seismic imaging of mid-crustal structure beneath central and eastern North America: possibly the elusive Grenville deformation? Geology 47, 371–374.

Manspeizer, W., DeBoer, J., Costain, J.K., Froelich, A.J., Coruh, C., Olsen, P.E., McHone, G.J., Puffer, J.H., Prowell, D.C., 1989. Post-Paelozoic activity. In: Hatcher Jr., R.D., Thomas, W.A., Viele, G.W. (Eds.), The Appalachian-Ouachita Orogen in the United States: The Geology of North America, vol. F-2, pp. 319–374.

Marzoli, A., Bertrand, H., Knight, K.B., Cirilli, S., Buratti, N., Vérati, C., Nomade, S., Renne, P.R., Youbi, N., Martini, R., Allenbach, K., Neuwerth, R., Rapaille, C., Zaninetti, L., Bellieni, G., 2004. Synchrony of the Central Atlantic magmatic province and the Triassic-Jurassic boundary climatic and biotic crisis. Geology 32 (11), 973–976.

Mazza, S.E., Gazel, E., Johnson, E.A., Kunk, M.J., McAleer, R., Spotila, J.A., Coleman, D.S., 2014. Volcanoes of the passive margin: the youngest magmatic event in eastern North America. Geology 42 (6), 483–486.

Menke, W., Lamoureux, J., Abbott, D., Hopper, E., Hutson, D., Marrero, A., 2018. Crustal heating and lithospheric alteration and erosion associated with asthenospheric upwelling beneath southern New England (USA). J. Geophys. Res., Solid Earth 123, 8995–9008. https://doi.org/10.1029/2018JB15921.

Murphy, B.S., Egbert, G.D., 2017. Electrical conductivity structure of southeastern North America: implications for lithospheric architecture and Appalachian topographic rejuvenation. Earth Planet. Sci. Lett. 462, 66–75.

Naif, S., 2018. An upper-bound on the conductivity of hydrated oceanic mantle at the onset of dehydration melting. Earth Planet. Sci. Lett. 482, 357–388.

Pommier, A., Le Trong, E., 2011. SIGMELTS: a web-portal for electrical conductivity calculations in geosciences. Comput. Geosci. 37 (9), 1450–1459. https://doi.org/10.1016/j.cageo.2011.01.002.

Pommier, A., Garnero, E.J., 2014. Petrology-based modeling of mantle melt electrical conductivity and joint interpretation of electromagnetic and seismic results. J. Geophys. Res., Solid Earth 119, 4001–4016. https://doi.org/10.1002/2013JB010449.

Pommier, A., Kohlstedt, D.L., Hansen, L.N., Mackwell, S., Tasaka, M., Heidelbach, F., Leinenweber, K., 2018. Transport properties of olivine grain boundaries from electrical conductivity experiments. Contrib. Mineral. Petrol. 173, 41. https://doi.org/10.1007/s00410-018-1468-z.

Porter, R., Liu, Y., Holt, W.E., 2016. Lithospheric records of orogeny within the continental U.S. Geophys. Res. Lett. 43, 144–153. https://doi.org/10.1002/2015GL066950.

Robinson, G.D., Healey, K., Kelly, V.C., 1988. Use of tourmaline in stream sediments to detect submarine exhalative sulfide deposits: example from central Virginia, USA. Appl. Geochem. 3 (2), 225–230.

Rychert, C.A., Rondenay, S., Fischer, K.M., 2007. P-to-S and S-to-P imaging of a sharp lithosphere-asthenosphere boundary beneath eastern North America. J. Geophys. Res. 112, B08314. https://doi.org/10.1029/2006JB004619.

Sandhaus, D.J., Craig, J.R., 1986. Gahnite in the metamorphosed stratiform massive sulfide deposits of the Mineral District, Virginia, USA. Mineral. Petrol. 35 (2), 77–98.

Schmandt, B., Lin, F.-C., 2014. P and S wave tomography of the mantle beneath the United States. Geophys. Res. Lett. 41, 6342–6349. https://doi.org/10.1002/2014GL061231.

Schultz, A., Egbert, G.D., Kelbert, A., Peery, T., Clote, V., Fry, B., Erofeeva, S., Staff of the National Geoelectromagnetic Facility and their contractors, 2006-2018. USArray TA magnetotelluric transfer functions. https://doi.org/10.17611/DP/EMTF/USARRAY/TA.

Steltenpohl, M.G., Zietz, I., Horton, J.W., Daniels, D.L., 2010. New York–Alabama lineament: a buried right-slip fault bordering the Appalachians and mid-continent North America. Geology 38 (6), 571–574.

Van der Lee, S., Regenauer-Lieb, K., Yuen, D.A., 2008. The role of water in connecting past and future episodes of subduction. Earth Planet. Sci. Lett. 273, 15–27.

Wagner, L.S., Fischer, K.M., Hawman, R., Hopper, E., Howell, D., 2018. The relative roles of inheritance and long-term passive margin lithospheric evolution on the modern structure and tectonic activity in the southeastern United States. Geosphere 14, 4. https://doi.org/10.1130/GES01593.1.

Wang, H., Currie, C.A., 2015. Magmatic expressions of continental lithosphere removal. J. Geophys. Res., Solid Earth 120, 7239–7260. https://doi.org/10.1002/2015JB012112.

Wannamaker, P.E., 2005. Anisotropy versus heterogeneity in continental solid earth electromagnetic studies: fundamental response characteristics and implications for physicochemical state. Surv. Geophys. 26, 733–765. https://doi.org/10.1007/s10712-005-1832-1.

Wannamaker, P.E., Hasterok, D.P., Johnston, J.M., Stodt, J.A., Hall, D.B., Sodergren, T.L., Pellerin, L., Maris, V., Doerner, W.M., Groenewold, K.A., Unsworth, M.J., 2008. Lithospheric dismemberment and magmatic processes of the Great Basin–Colorado Plateau transition, Utah, implied from magnetotellurics. Geochem. Geophys. Geosyst. 9.